13. G. Baffou, R. Quidant, and F. J. García de Abajo, "Nanoscale control of optical heating in complex plasmonic systems," ACS Nano **4**(2), 709–716 (2010).
14. P. Zijlstra, J. W. M. Chon, and M. Gu, "White light scattering spectroscopy and electron microscopy of laser induced melting in single gold nanorods," Phys. Chem. Chem. Phys. **11**(28), 5915–5921 (2009).
15. Z. Qin and J. C. Bischof, "Thermophysical and biological responses of gold nanoparticle laser heating," Chem. Soc. Rev. **41**(3), 1191–1217 (2012).
16. A. O. Govorov, W. Zhang, T. Skeini, H. Richardson, J. Lee, and N. A. Kotov, "Gold nanoparticle ensembles as heaters and actuators: melting and collective plasmon resonances," Nanoscale Res. Lett. **1**(1), 84–90 (2006).
17. A. M. Gobin, M. H. Lee, N. J. Halas, W. D. James, R. A. Drezek, and J. L. West, "Near-infrared resonant nanoshells for combined optical imaging and photothermal cancer therapy," Nano Lett. **7**(7), 1929–1934 (2007).
18. W. Zhao and J. M. Karp, "Tumour targeting: nanoantennas heat up," Nat. Mater. **8**(6), 453–454 (2009).
19. P. K. Jain, I. H. El-Sayed, and M. A. El-Sayed, "Au nanoparticles target cancer," Nano Today **2**(1), 18–29 (2007).
20. D. Boyer, P. Tamarat, A. Maali, B. Lounis, and M. Orrit, "Photothermal imaging of nanometer-sized metal particles among scatterers," Science **297**(5584), 1160–1163 (2002).
21. S. Berciaud, D. Lasne, G. A. Blab, L. Cognet, and B. Lounis, "Photothermal heterodyne imaging of individual metallic nanoparticles: theory versus experiment," Phys. Rev. B **73**(4), 045424 (2006).
22. D. Lasne, G. A. Blab, S. Berciaud, M. Heine, L. Groc, D. Choquet, L. Cognet, and B. Lounis, "Single nanoparticle photothermal tracking (snapt) of 5-nm gold beads in live cells," Biophys. J. **91**(12), 4598–4604 (2006).
23. G. Baffou, M. P. Kreuzer, F. Kulzer, and R. Quidant, "Temperature mapping near plasmonic nanostructures using fluorescence polarization anisotropy," Opt. Express **17**(5), 3291–3298 (2009).
24. A. G. Skirtach, C. Dejugnat, D. Braun, A. S. Susha, A. L. Rogach, W. J. Parak, H. Möhwald, and G. B. Sukhorukov, "The role of metal nanoparticles in remote release of encapsulated materials," Nano Lett. **5**(7), 1371–1377 (2005).
25. D. Pissuwan, S. M. Valenzuela, and M. B. Cortie, "Therapeutic possibilities of plasmonically heated gold nanoparticles," Trends Biotechnol. **24**(2), 62–67 (2006).
26. L. Cao, D. N. Barsic, A. R. Guichard, and M. L. Brongersma, "Plasmon-assisted local temperature control to pattern individual semiconductor nanowires and carbon nanotubes," Nano Lett. **7**(11), 3523–3527 (2007).
27. H. M. Pollock and A. Hammiche, "Micro-thermal analysis: techniques and applications," J. Phys. D Appl. Phys. **34**(9), R23–R53 (2001).
28. G. L. Liu, J. Kim, Y. Lu, and L. P. Lee, "Optofluidic control using photothermal nanoparticles," Nat. Mater. **5**(1), 27–32 (2006).
29. V. Garcés-Chávez, R. Quidant, P. J. Reece, G. Badenes, L. Torner, and K. Dholakia, "Extended organization of colloidal microparticles by surface plasmon polariton excitation," Phys. Rev. B **73**(8), 085417 (2006).
30. X. Miao, B. K. Wilson, and L. Y. Lin, "Localized surface plasmon assisted microfluidic mixing," Appl. Phys. Lett. **92**(12), 124108 (2008).
31. A. O. Govorov and H. H. Richardson, "Generating heat with metal nanoparticles," Nano Today **2**(1), 30–38 (2007).
32. P. B. Johnson and R. W. Christy, "Optical constants of the noble metals," Phys. Rev. B **6**(12), 4370–4379 (1972).
33. U. Kreibig and M. Vollmer, *Optical Properties Of Metal Clusters* (Springer, 1995).
34. S. A. Maier, *Plasmonics: Fundamentals and Applications* (Springer Verlag, 2007), Chap. 5.
35. Y. Yue and X. Wang, "Nanoscale thermal probing," Nano Reviews **3**: 11586 - DOI: 10.3402/nano.v3i0.11586 (2012)
36. E. R. G. Eckert and R. M. Drake, *Heat and Mass Transfer* (McGraw-Hill, 1959).
37. F. Cooper, "Heat transfer from a sphere to an infinite medium," Int. J. Heat Mass Tran. **20**(9), 991–993 (1977).

1. Introduction

Noble metal nanoparticles are well known as efficient light scatterers and absorbers owing to their strong interactions with visible and infrared light through localized plasmon resonances. When two metal nanoparticles are placed in close proximity, their plasmon modes can be coupled via the near-field interaction and the plasmon resonance shows a distance-dependent characteristic [1–6]. A plasmon ruler can be created on the basis of this effect, which is capable of monitoring nanoscale distances and distance changes during transient biological processes and molecular activities like DNA hybridization in biological systems [7–10], Spectrum-based plasmon rulers have been under intense investigation in recent years. Jain *et al.* [9] and Su *et al.* [5] demonstrated the scaling behavior of the distance-dependent characteristics of spectral shift and obtained a universal plasmon ruler equation. Reinhard *et al.* [8] experimentally evaluated the advantages and limitations of this approach and calibrated the ruler using 42- and 87-nm-diameter particle pairs. Liu *et al.* [11] designed a coupled plasmonic oligomer whose scattering spectra can be used to retrieve three-dimensional configuration information of a nanostructure.

Apart from scattering, an optically excited nanoparticle can be heated through dissipation of absorbed light into resistive thermal energy [12–14]. Plasmon enhanced metal nanoparticles can be used as efficient and flexibly controllable nanosources of heat [15,16] and have shown exciting potential applications including photothermal cancer therapy [17–19], biological imaging and spectroscopy [20–23], drug delivery [24,25], nanocatalysis [26,27] as well as nanofluidics [28–30].

In this paper we demonstrate that the distance-dependence of the thermal response of an optically heated metal nanoparticle pair can also be used to create a nanoscale ruler. This distance-dependent effect results from two mechanisms [31]. On one hand, since the particles are coupled through near-field interaction, the absorption power depends on the interparticle distance and the incident light polarization. On the other hand, due to the heat flux generated by the neighboring particle, the heating effect (temperature increase in our case) of each particle is enhanced compared to single particle and this accumulative heating effect is also distance-dependent. For the thermal ruler to be of practical use, quantitative and systematic studies are essential on the particle temperature increase as a function of the interparticle distance. We conduct numerical simulations on light absorption and heat-transfer in a gold nanoparticle dimer system using the finite-element method (FEM). Our simulations show that the absorption power at a fixed wavelength for polarization along the interparticle axis exhibits an exponential-like decay with the interparticle gap. The exponential decay of absorption power with the interparticle gap becomes size-independent when the absorption power and the gap are scaled respectively by the single particle absorption power and the particle diameter. This scaling behavior can be qualitatively explained using a simple dipolar-coupling model. Based on this scaling behavior of absorption power, we further derive a scaling behavior for the temperature increase of each particle in a nanoparticle dimer system using the thermal diffusion law and it is verified by simulation data. A ruler equation is then established relating the particle temperature and the interparticle distance.

2. Light absorption

Interaction of light with gold nanoparticles is modeled using the previously reported method using commercially available FEM solver COMSOL Multiphysics [12]. Absorbed heat power P by a nanostructure is obtained by integrating heat density Q_d over that structure. Experimental data from Johnson and Christy [32] with cubic spline interpolation are used throughout this study for the permittivity of gold.

The evolution of the absorption power spectrum of a gold nanoparticle dimer (Fig. 1(a)) with respect to the interparticle edge-to-edge distance (gap) s is presented in Fig. 1(b) and Fig. 1(c). The dimer is composed of two identical gold nanospheres with diameters $D = 50$ nm immersed in water (refractive index $n = 1.33$). The illumination light intensity is 1 mW/μm^2, a typical value used for nanoparticle absorption studies. The absorption power of each particle in the dimer is identical due to the symmetric configuration of the system. Note that the absorption power in the paper refers to that of each individual nanoparticle. Figure 1(b) corresponds to the situation where the polarization direction of incident light is parallel to the interparticle axis and Fig. 1(c) is for polarization direction perpendicular to the axis. Similar to the scattering and extinction spectra, the absorption spectra behave quite differently for the two polarization directions. For parallel polarization, the peak absorption wavelength strongly red-shifts and heating effect is significantly enhanced as the interparticle distance is reduced. On the contrary, the absorption maximum slightly blue-shifts and absorption is slightly suppressed with decreasing distance for perpendicular polarization. This is in agreement with the observations by Govorov *et al.* [16]. The wavelengths in this paper refer to free-space wavelengths in all cases. The resonance shift is attributed to the electromagnetic coupling of the single-particle plasmons, and the polarization and distance dependence can be explained on the basis of a simple dipole-dipole coupling model [1]. We shall be interested in parallel polarization in this work which produces larger variations in heating effect owing to stronger plasmon coupling.

From the absorption spectra for various gaps (Fig. 1(b)) we see that energy absorption of each nanoparticle in the dimer decays with interparticle gap in a certain range under illumination of a monochromatic light source whose wavelength is beyond the peak absorption wavelength. For example, if we set the free-space wavelength of the excitation plane wave to be 585 nm (the absorption maximum for s = 4 nm), the absorption power is supposed to decay monotonously with the interparticle gap for interparticle gaps larger than 4 nm, which is plotted in Fig. 1(d). The decay can be fit very closely to an exponential decay with a decay length of 10.9 ± 2.1 nm.
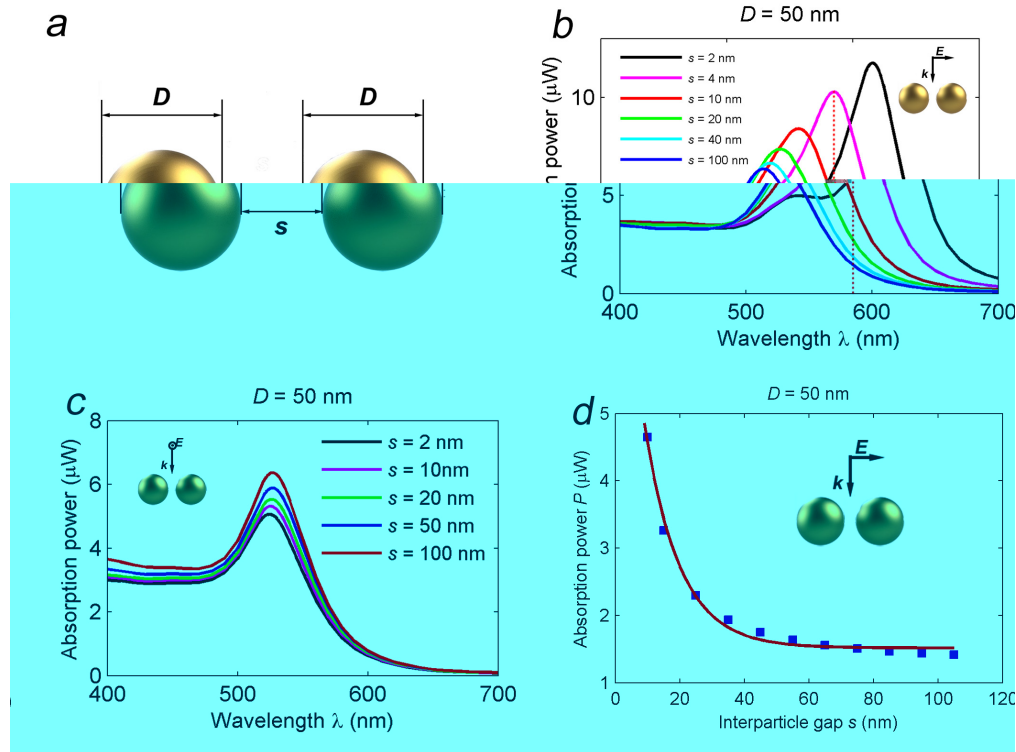

Fig. 1. Light absorption of a gold sphere dimer versus interparticle gap. (a) Sketch of the dimer. (b,c) Absorption spectra of gold nanosphere dimers of varying interparticle gap for incident light polarized (b) parallel and (c) perpendicular to the interparticle axis. (d) Absorption power of each sphere in the gold sphere dimer as a function of interparticle gap for light polarization direction parallel to the interparticle axis. The red curve is least-square fit to exponential decay $P = P_0 + a\, e^{-s/l}$, and the decay length l is 10.9 ± 2.1 nm. The incident light intensity is 1 mW/µm².

3. Scaling behavior

Su *et al.* [5] and Jain *et al.* [9] observed that the plasmon resonance shift has "universal scaling behavior", which indicates that for parallel polarization the peak shift decays nearly exponentially with increasing interparticle gap and the exponential decay becomes size-independent if the shift and gap are scaled respectively by the single-particle resonance wavelength and the particle size. Moreover, the effects of particle shape, metal type and medium dielectric constant on the decay constant are weak. A plasmon ruler equation [9] is thus deduced, which is a useful guide for designing spectrum-based plasmon rulers.

Inspired by the scaling behavior of plasmon shift, we study the absorption power of individual nanoparticle in a particle dimer immersed in water under parallel polarization illumination as a function of the ratio of the interparticle gap scaled by the particle diameter for spherical nanoparticles of different sizes (D = 30, 40, 50 nm). Particles of these sizes are

appropriate for making a nanoruler with tiny influence on the system to be measured while providing sufficiently intense light absorption. The wavelength is fixed at 585 nm and the flux of the incident light is 1 mW/μm². The absorption power P is scaled by P_0, which is the absorption power of single nanoparticle with respective diameters. The ratio P/P_0 can be seen as the enhancement of absorption over single particle due to plasmon coupling and thus reflects the coupling strength. While the decays of absorption power for different particle sizes follow different curves with different decay lengths, all data points fall on the same curve after this scaling. The scaling behavior can be described by

$$\frac{P}{P_0} = a \exp\left(-\frac{s/D}{\tau}\right) + 1,$$ (1)

where a is the amplitude of the decay and τ is the decay constant. A least-square fit using the data in Fig. 2 leads to $a = 5.9 \pm 0.7$ and $\tau = 0.19 \pm 0.02$.
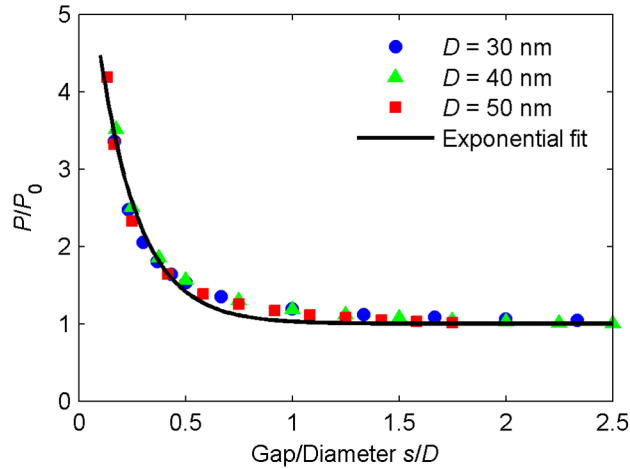

Fig. 2. Absorption enhancement versus gap-diameter ratio. The data is exponentially fit with the parameters of $a = 5.9 \pm 0.7$ and $\tau = 0.19 \pm 0.02$.

4. Dipolar-coupling model

In order to acquire a further understanding of the scaling behavior of distance decay of light absorption in metal nanoparticle dimers, we carried out theoretical calculations based on the dipole-dipole interaction model [33].

The electric dipole moment **p** of a small particle in an electric field **E** is

$$\mathbf{p} = \varepsilon_0 \varepsilon_m \alpha \mathbf{E},$$ (2)

where ε_0 is the vacuum permittivity, ε_m the medium dielectric constant and α the (complex) dipole polarizability of an isolated metal nanoparticle of sub-wavelength diameter in the quasistatic approximation. For spherical nanoparticles, α can be written as [34]

$$\alpha = \frac{1}{2}\pi D^3 \frac{\varepsilon - \varepsilon_m}{\varepsilon + 2\varepsilon_m},$$ (3)

where $\varepsilon = \varepsilon_r + i\varepsilon_i$ is the dielectric function of the metal. In the dimer, the electric field on each particle is the sum of the incident light field **E** and the near-field of the neighboring particle [9]:

$$\mathbf{E}' = \mathbf{E} + \frac{\kappa \mathbf{p}'}{4\pi\varepsilon_m \varepsilon_0 d^3}.$$ (4)

In the above equation, $\mathbf{p}'$ is the polarizability of each particle in the dimer. κ is an orientation factor, which depends on the alignment of the two single-particle dipoles. $\kappa = 2$ is for dipoles arranged head-to-tail corresponding to parallel polarization in our experiments, while $\kappa = -1$ for dipoles aligned side-by-side corresponding to perpendicular polarization. d is the center-to-center distance between particles. From Eqs. (2)(3)(4) and considering $\mathbf{p}' = \alpha \varepsilon_0 \varepsilon_m \mathbf{E}' = \alpha' \varepsilon_0 \varepsilon_m \mathbf{E}$, the net polarizability α' of each particle in the dimer is given as

$$\alpha' = \frac{\alpha}{1 - \dfrac{\alpha}{2\pi d^3}} = \frac{2\pi D^3 (\varepsilon - \varepsilon_m)}{\varepsilon \left[4 - \left(\dfrac{D}{d} \right)^3 \right] + \varepsilon_m \left[8 + \left(\dfrac{D}{d} \right)^3 \right]}. \tag{5}$$

Absorption power of a nanoparticle is $P = C_{abs} I_0$, where $C_{abs} = k\mathrm{Im}[\alpha]$ is the absorption cross-section and I_0 is the light intensity. Then the absorption enhancement over single particle due to plasmon coupling can be expressed as (Notice that $d = s + D$)

$$\frac{P}{P_0} = \frac{16 \left[(\varepsilon_r + 2\varepsilon_m)^2 + \varepsilon_i^2 \right]}{\left\{ \left[4 - \left(\dfrac{1}{1 + s/D} \right)^3 \right] \varepsilon_r + \left[8 + \left(\dfrac{1}{1 + s/D} \right)^3 \right] \varepsilon_m \right\}^2 + \left[4 - \left(\dfrac{1}{1 + s/D} \right)^3 \right]^2 \varepsilon_i^2}. \tag{6}$$

In Eq. (6) ε_r and ε_i are respectively the real and imaginary part of the metal dielectric constant. ε_m is the dielectric constant of the surrounding medium and it relates to refractive index through $\varepsilon_m = n_m^2$. ε_r and ε_i are constants as long as the wavelength of the incident light is fixed. Equation (6) shows that the absorption enhancement P/P_0 is a rational function of gap-diameter ratio s/D, which can be approximated to an exponential decay without significant loss in accuracy (Fig. 3).

However, the estimated a value of 2.0 is smaller than that observed in the FEM simulations and τ value of 0.3 is larger than the simulation results. In line with previous observations [9], the dipole-coupling model underestimates the amplitude and the decay rate of particle absorption especially in the case of very small interparticle separations as higher-order interactions take increasingly important roles. Nevertheless, the distance decay and scaling behavior of absorption can be qualitatively understood on the basis of the dipolar model.
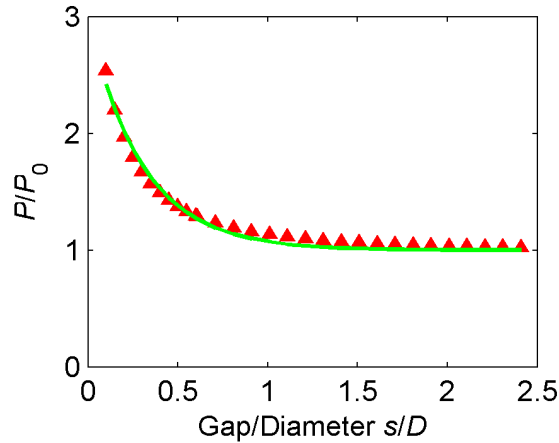

Fig. 3. Plot of the absorption enhancement as a function of gap/diameter calculated using the dipolar-coupling model (Eq. (6)) for a gold nanosphere pair system in water ($n = 1.33$) under parallel polarization, i.e. $\kappa = 2$. The green solid curve is the least-square fit to the single exponential decay $y = a \cdot e^{-x/\tau}$, where $\tau = 0.30 \pm 0.02$ and $a = 2.0 \pm 0.2$.

5. Temperature change and plasmon ruler equation

We have shown that the light absorption power for parallel polarization decays approximately exponentially with interparticle gap. However, since energy dissipation is very difficult to measure experimentally, it is not practical to make a plasmon ruler on the basis of the distance dependence of absorption power. A direct consequence of optical heating is the temperature increase of the metallic nanoparticles and the medium around the particles on account of heat diffusion. The temperature of each nanoparticle in the particle dimer is related to their absorption power and thus also reflects the interparticle distance. Though the temperature of a structure in the nanoscale (like a nanoparticle in our case) is difficult to be measured directly, quite a few techniques for indirect nanoscale temperature probing have been developed in recent years, which are well summarized in literatures [15, 35]. Here our main interest is in the temperature at the surface of an optically heated nanoparticle at steady state, for the transient temperature measurement is rather complicated and also unnecessary for our purpose.

Baffou et $al.$ [13] derived the expression for the steady-state profile of temperature increase in a single-particle-medium system with the nanosphere being a steady optically driven heat source by relating the temperature increase to the electrostatic potential around a uniformly charged sphere:

$$\Delta T\left(r\right)=\begin{cases}\dfrac{P}{4\pi\kappa_\mathrm{m}R},r<R,\\[2ex]\dfrac{P}{4\pi\kappa_\mathrm{m}r},r>R.\end{cases}\tag{7}$$

In the above equation P is the absorption power of the particle, R the particle radius and κ_m the thermal conductivity of the medium. $\Delta T(r)$ shows an inverse proportional dependence on the distance to the particle center in the surrounding medium while the temperature inside the gold nanoparticle is nearly uniform since the thermal conductivity of gold is much higher than that of the medium [13]. According to the electrostatic analogy, values of temperature increase should be added like Coulomb potential if more than one heat sources exist in a system. Thus if the heat power produced by each nanoparticle in the dimer system mentioned above is P, then the temperature increase of each nanoparticle can be written as

$$\Delta T_\mathrm{NP}=\frac{P}{4\pi\kappa_\mathrm{m}}\left(\frac{1}{R}+\frac{1}{d}\right)=\frac{P}{4\pi\kappa_\mathrm{m}}\left(\frac{2}{D}+\frac{1}{s+D}\right).\tag{8}$$

Equation (8) indicates that ΔT_NP of each particle results from the superposition of the heating effects of its own light absorption and the heating of the neighboring identical heat source.

To validate Eq. (8), we conduct FEM simulations on the thermal response of the nanoparticle dimer. Figure 4 shows the simulation results of temperature increase of each nanoparticle (D = 50 nm) compared with calculation results using Eq. (8) against the interparticle gap. The absorption power of each particle is 20 µW for all interparticle distances and the dimer is in water (κ_water = 0.6 Wm^{-1}K^{-1}). Larger and smaller nanoparticles are also studied (results not shown here) and we observe that simulation and calculation results are in very good agreement, with relative errors not exceeding 5% for all particle sizes. Simulation and calculation values exhibit larger differences for narrower gap and larger particles, which may be attributed to the derivation from the assumption that the particles are point heat sources [36].
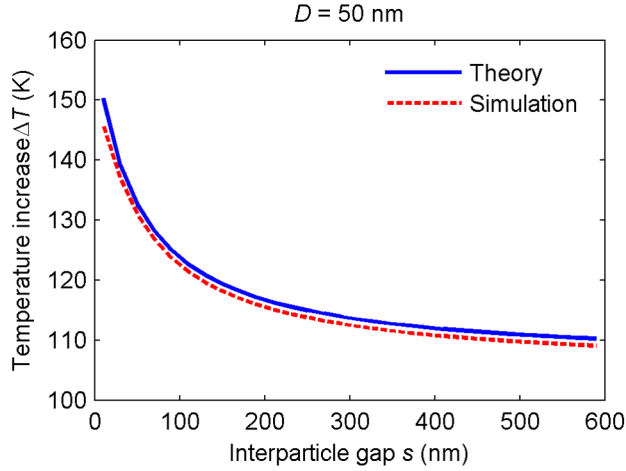
Fig. 4. Temperature increase versus interparticle distance between two 50 nm diameter gold nanospheres: comparison of Eq. (8) with the FEM simulation. The heat power of each sphere is 20 μW.

Combining Eqs. (1), (7) and (8) we obtain the expression for the temperature increase of each spherical nanoparticle ΔT_{NP} versus interparticle gap s under monochromatic light illumination

$$\frac{\Delta T_{NP}}{\Delta T_{NP}^{0}} = \left[a\exp\left(-\frac{s/D}{\tau}\right)+1 \right]\left[1+\frac{1}{2(s/D+1)} \right],\qquad(9)$$

where ΔT_{NP}^{0} is the steady-state temperature increase of single nanosphere under light illumination of the same wavelength.

We further calculate particle temperature increase corresponding to the absorption power in Fig. 2 for various particle sizes. As expected, all data points fall on a same curve when ΔT_{NP} and s are respectively scaled by ΔT_{NP}^{0} and D (Fig. 5). In Fig. 5, the solid black line is the least-square fit to Eq. (9) using the simulation data, which yields $a = 6.1 \pm 0.8$ and $\tau = 0.17 \pm 0.02$. These two constants agree with the constants fitted to Eq. (1) above, which verifies Eq. (9).

A temperature-based plasmon ruler can thus be created with Eq. (9) as the ruler equation. Parameters a and τ can be calibrated experimentally.

Under CW light illumination, the relaxation time τ_e for a gold nanosphere in medium to reach steady-state temperature can be estimated [12,37] with $\tau_e = D^2/4\alpha$, where α is the thermal diffusivity of the water and its value [12] is 1.435×10^{-7} m^2/s. The τ_e of a 50 nm diameter sphere is estimated to be 4.35 ns. Therefore, the thermal response of the nanoruler is rather fast, with negligible time delay during a dynamic distance-change process.
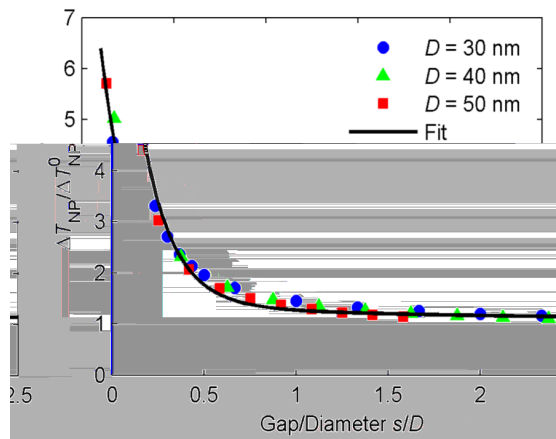
Fig. 5. Temperature increase enhancement versus gap-diameter ratio and exponential fit with $a =$ 6.1 ± 0.8 and $\tau = 0.17 \pm 0.02$.

6. Perpendicular polarization

Contrary to the case with light polarized parallel to the interparticle axis, light absorption is slightly enhanced for increasing interparticle distance under perpendicular polarization illumination (Fig. 1(c)). Considering the inverse proportional rule of temperature increase with respect to interparticle distance (Eq. (7)), the temperature of the particle will not necessarily evolve monotonously with distance. A typical result corresponding to this case is shown in Fig. 6, which shows that the particle temperature changes within a small range, and one value of particle temperature corresponds to several values of distance, which is disadvantageous for making a plasmon ruler.
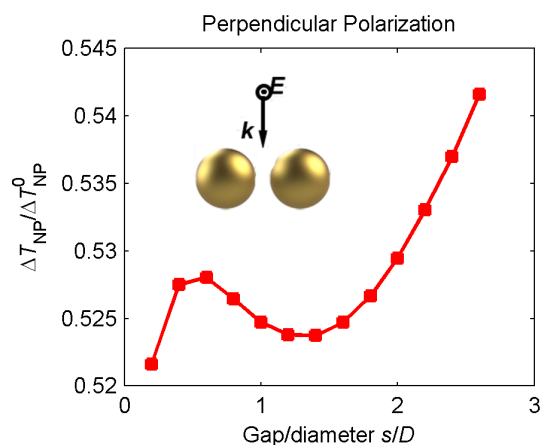

Fig. 6. Plot of temperature increase versus interparticle gap of a 50 nm diameter Au nanosphere dimer for perpendicular polarization. The intensity and wavelength of the incident light are respectively 1 mW/μm² and 530 nm.

7. Conclusion

Temperature response of an optically heated gold nanoparticle pair is numerically modeled to explore the possibility of creating a nanoscale plasmon ruler based on the distance dependence of the particle temperature change. The absorption power at a fixed incident wavelength for polarization along the interparticle axis is found to decay nearly exponentially with respect to interparticle gap. In addition, the exponential decay of absorption power with the interparticle gap becomes size-independent when the absorption power and the gap are scaled respectively

by the single particle absorption power and the particle diameter. This scaling behavior is then qualitatively explained on the basis of a simple dipolar-coupling model. We further found the scaling behavior of the steady-state temperature of each particle in a spherical nanoparticle dimer system and a ruler equation is established for the temperature-based nanoscale ruler. Our quantitative results can be a useful guide for designing and optimizing temperature-based plasmon rulers. The method presented can be valuable for quantitatively studying photothermal effects in various plasmonic nanostructures, which can find applications in biological sensing and imaging, optical data storage and photovoltaic technology.

Acknowledgments